DNA Base Pair Stacks with High Electric Conductance: A Systematic Structural Search

Yuri A. Berlin,[†] Alexander A. Voityuk,[‡,§] and Mark A. Ratner[†,*]

[†]Department of Chemistry, Northwestern University, 1145 Sheridan Road, Evanston, Illinois 60208-3113, United States , [‡]Institució Catalana de Recerca i Estudis Avançats (ICREA), Barcelona, Spain, and [§]Institut de Química Computational, Universitat de Girona, 17071 Girona, Spain

ABSTRACT

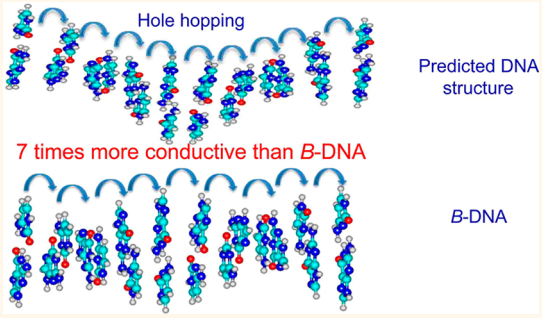

We report a computational search for DNA π-stack structures exhibiting high electric conductance in the hopping regime, based on the INDO/S calculations of electronic coupling and the method of data analysis called k-means clustering. Using homogeneous poly(G)—poly(C) and poly(A)—poly(T) stacks as the simplest structural models, we identify the configurations of neighboring G:C and A:T pairs that allow strong electronic coupling and, therefore, molecular electric conductance much larger than the values reported for the corresponding reference systems in the literature. A computational approach for modeling the impact of thermal fluctuations on the averaged dimer structure was also proposed and applied to the [(G:C),(G:C)] and [(A:T),(A:T)] duplexes. The results of this work may provide guidance for the construction of DNA devices and DNA-based elements of nanoscale molecular circuits. Several factors that cause changes of step parameters favorable to the formation of the predicted stack conformation with high electric conductance of DNA molecules are also discussed; favorable geometries may enhance the conductivity by factors as large as 15.

KEYWORDS: DNA · π-stack · step parameters · molecular conductance · electronic coupling

Interest in using deoxyribonucleic acid (DNA) as a building block for nanoelectronic devices originates from two important properties of this molecule. One property is the ability of DNA to be organized into predictable nanometer-sized structures in both two and three dimensions. This remarkable feature has been exploited to obtain a variety of individual constructs including a cube-like molecule, a DNA-truncated octahedron, DNA origami, two- and three-dimensional crystalline arrays (for review, see *e.g.*, ref 1) and spherical DNA.[2] The successful assembling of such molecular objects and the subsequent design, formation, and structural evaluation of various unusual DNA motifs clearly demonstrate that DNA has great potential as a "bottom-up" construction material for making nanoscale templates and machines.[3−5]

Another property that makes DNA a promising candidate for a number of applications in molecular electronics is the possibility to conduct electric current[6−9] transporting charge carriers ("electronic" holes) over distances as large as 40−200 Å.[10−19] This, together with the relative ease to form various constructs, enables one to consider DNA as an interesting compound for the design of nanoelectronic circuits.[20,21] For that reason (as well as for the biological relevance), processes of hole transfer and transport in DNA have been the subjects of extensive research efforts over almost three decades (for comprehensive overview of the field, see *e.g.*, refs 22−25). These efforts have shown that the stacked base pairs inside the double helix provide the pathway for the long-distance charge transport along a DNA molecule, and that the motion of a positive charge primarily generated inside the π-stack array on a particular guanine (G) site could usually be treated as a series of short-range hops between neighboring Gs.[18,26−30] Within this mechanistic picture, each single G is a stepping stone for hole transport, since this base has the lowest oxidation potential among the four native nucleobases.[31−33] Thus, according to current consensus, the process of hole migration along stacks consisting of guanine:cytosine (G:C) base pairs linked by adenine:thymine (A:T) bridges is viewed as a series of steps of variable lengths determined by the distance, *R*, between neighboring Gs (the so-called G-hopping[19]). Each elementary step of this multistep motion proceeds *via* tunneling

* Address correspondence to ratner@northwestern.edu.

Received for review June 28, 2012 and accepted August 18, 2012.

Published online August 18, 2012
10.1021/nn3030139

or by thermal activation. The former mechanism is characterized by strong (exponential) dependence of the charge transfer rate k_{CT} on R, in contrast to the mechanism of thermal activation, which usually exhibits small variations of k_{CT} values with R, such as $a/(1 + bR)$ dependence. As a consequence, the tunneling channel is dominant for bridges with a length of at most four A:T base pairs, while the mechanism of thermal activation prevails for longer bridges.[19,34−37]

The transition from tunneling to thermally activated hopping regime was observed not only for charge transfer in DNA, but also for the zero-bias electric conductance g of various molecular wires connecting two electrodes.[38−42] This suggests that the same transport mechanisms govern both phenomena in DNA as well as in other systems. Therefore it can be expected that for a particular wire, g and k_{CT} should be closely related. Indeed, for a given molecule, Nitzan *et al.*[43−45] have derived a relationship between the charge transfer rate and the zero-bias molecular conductance in the coherent tunneling regime. Their analysis has been extended to the particular case of hopping with equal transition rates for all successive elementary steps.[46,47] The relation between k_{CT} and g was also obtained, beyond this limitation, for a fairly general form of the energy landscape governing hopping motion.[48]

It should be noted that relations derived in all these cases become remarkably simple if one neglects the distinction between the rates to depopulate the stack of base pairs in two situations, where the same stack (i) links donor and acceptor species and (ii) connects two metallic electrodes. Then for sufficiently high temperature, we obtain the following numerical estimate[45,46,48]

$$g(\Omega^{-1}) \approx 5 \times 10^{-18} k_{CT}(s^{-1}) \quad (1)$$

This estimate is valid when the thermal energy k_BT exceeds the difference $\Delta E = E_{FB} - E_{BD}$ with E_{FB} denoting the energy spacing between the Fermi level of leads and the bridge level, while E_{BD} is the energy gap between the bridge and the donor state.

Equation 1 predicts that the conductance of DNA should be sequence-dependent since the rate of the hole transfer process was found to vary with base pair sequences.[10,13,15,49,50] For instance, in sequences containing G:C and A:T pairs a hole can be transferred between G-C base-pairs separated by more than three A:T base-pairs *via* a thermally induced hopping mechanism.[19,34,35] However the hole transfer in such systems proceeds quite slowly ($<10^5$ s^{-1}).[51−54] Certainly this limits the potential applications of DNA as a conducting molecule in molecular-scale devices since for stacks involving both G:C and A:T pairs, the g values are expected to be less than 0.5 pS according to eq 1. Although hole transfer occurs rapidly along A_3G_n diblock polypurine sequences with $n = 1-19$ ($k_{CT} < 2 \times 10^9$ s^{-1})[55] and along A-tracts with up to seven A:T pairs (10^8 s^{-1} $< k_{CT} < 2 \times 10^{11}$ s^{-1}),[36,37] the molecular conductance in these two systems remains quite low[47,56] and does not exceed 10 nS and 1 μS, respectively.

On the basis of these experimental data and numerical estimates, we conclude that natural DNA is a poor electrical conductor and that its molecular conductivity must be substantially improved to be sufficient for applications in nanoelectronics. Owing to its many possible structural manipulations, DNA offers opportunities to reach larger conductance without doping and without invoking other methods for chemical modifications of base pair stacks.[21] Recent theoretical studies[57−62] dealing with the effects of structural fluctuations in DNA on two key parameters controlling the hole transfer rate (electronic coupling and site energies) strongly support these expectations. In particular, the results of quantum chemical calculations and molecular dynamics simulations[57] suggest that the calculated electronic coupling is very sensitive to variations of the positions of the Watson−Crick pairs. Since k_{CT} for hole transfer is proportional to the square of the coupling matrix element,[35,63−65] such structural changes can alter the transfer rates by factors of 10^2-10^8 for different reasonable conformations of two neighboring A:T nucleobases. By contrast, weaker conformational dependence is predicted for both the site energies[66] and the reorganization energy[67] for hole transfer.

In this paper we develop a computational methodology for searching for DNA structures with strong electronic coupling and therefore with large mobility of charge carriers and high zero-bias intramolecular conductance in the regime of sequential hopping. This methodology combines the very efficient and quite accurate INDO/S method for quantum mechanical calculations of electronic coupling[68] with the data analysis technique known as k-means clustering.[69,70] Using this methodology, we identify structures of homogeneous poly(A)−poly(T) and poly(G)−poly(C) stacks with zero-bias intramolecular conductance significantly larger than for conventional B-DNA. Corrections of the averaged [(G:C),(G:C)] and [(A:T),(A:T)] dimer structures for thermal fluctuations were also calculated and are briefly discussed. The optimal structures occurring through thermal fluctuations suggest new structural targets for synthesis of new DNA stacks with substantially (5-fold or more) increased conductance.

RESULTS AND DISCUSSION

Before proceeding to the identification of dimer structures which provide high electric conductance in the regime of sequential hopping, one should verify that such conductive structures of [(G:C),(G:C)] and [(A:T),(A:T)] duplexes do exist and that they make a significant contribution to the mean of V^2. This is done by computing the distribution of the number of dimer structures $n(V^2)$ over the electronic coupling squared V^2. Then the number of dimers $N(V^2 > V^2_{max})$ with V^2

greater than a certain value V^2_{max} is given by

$$N(V^2 > V^2_{max}) = \int_{V^2_{max}}^{\infty} n(V^2)\, dV^2 \qquad (2)$$

where V^2_{max} is the upper limit of the electronic coupling for the given subset of configurations with V^2 defined as

$$\langle V^2 \rangle = \int_0^{V^2_{max}} V^2 n(V^2)\, dV^2 \qquad (3)$$

To avoid confusion, we note that $n(V^2)$ has units of $1/V^2$, so that by virtue of eq 2 $N(V^2 > V^2_{max})$ is the dimensionless quantity.

An example of the distribution $n(V^2)$ for the particular case of the [(G:C),(G:C)] dimer is shown in Figure 1.

As evident from the data obtained by numerical integration of eq 2, $N(V^2 > V^2_{max})$ for [(G:C),(G:C)] structures drops very fast as V^2_{max} increases. In particular, the number of dimer configurations with electronic coupling squared larger than V^2_{max} = 0.005, 0.01, 0.05, and 0.1 $(eV)^2$ is found to be ~20%, 12%, 1.3%, and 0.2% of the total number of randomly generated configurations, respectively. Only 12% of all dimer configurations have the V^2 values that exceed $V^2 = 0.0065$ $(eV)^2$ deduced for the reference structure.[71] Moreover, since conductance in eq 1 linearly increases with k_{CT} while the latter quantity is usually proportional to V^2,[72,73] the zero bias g value for [(G:C),(G:C)] dimer is expected to decrease approximately by 30% if only about 2% of all configurations, that is, the structures with $V^2 \geq 0.04$ $(eV)^2$, are excluded from consideration (see Figure 2).

Note also that according to the data shown in Figure 2, the average conductance should fall by a factor of 3.5 if we neglect 10% of configurations with the strongest (>0.01 $(eV)^2$) electronic coupling squared for two neighboring G bases. Thus, a remarkable enhancement of transport properties of base pair stacks with homogeneous sequences can be achieved using a relatively small number of conformations with the proper structures providing the strongest electronic coupling. Such structures of [(G:C),(G:C)] and [(A:T),(A:T)] dimers together with the values of step parameters will be specified in subsequent sections.

Highly Conductive [(G:C),(G:C)] Dimer Structures. To find out how the zero-bias electric conductance g depends on the structure of [(G:C),(G:C)] dimer duplexes in the regime of sequential hopping, V^2 (linearly related to g) was calculated at various randomly selected twist, shift, and slide. The scatter plot of the electronic coupling squared *versus* the values of these three step parameters is presented in Figure 3. Twist turns out to be smaller than 50° for all structures with strong coupling ($\geq$0.04 $(eV)^2$, see highlighted region). The values of base pair translations in these structures may vary within wide limits ranging from −1 Å up to +3 Å for shift and from −1 Å up to 2.5 Å for slide, excluding in the latter case the narrow interval between 1.5 and 2.5 Å.

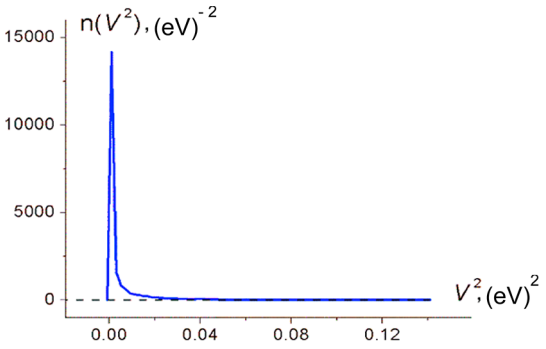

Figure 1. Distribution of the number of dimer structures $n(V^2)$ as a function of the electronic coupling squared V^2.

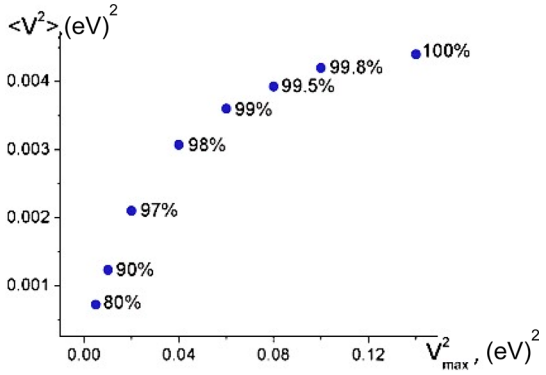

Figure 2. Variations of the mean V^2 defined by eq 3 for various subsets of configurations differing by the upper limit V^2_{max} of the electronic coupling squared. Numbers near the data points are the percentage of all configurations with the mean value of the electronic coupling squared V^2 shown on the vertical axis.

For further analysis, 6097 dimer configurations with twist ≤50° were selected from 22 000 randomly generated structures. The average V^2 over this data subset is $\langle V^2 \rangle \geq 0.012$ $(eV)^2$. Thereafter the selected configurations were divided into 20 groups using the k-means clustering algorithm.[74]

Characteristics of four representative clusters with electronic coupling squared $V^2_{cl} \geq 0.030$ $(eV)^2$ are given in Table 1.

The structures with the largest V^2_{cl} and therefore with the highest molecular conductance are contained in cluster A. For that group of structures, V^2_{cl} is about 0.1 $(eV)^2$, that is, 15 times larger than the average value $\langle V^2 \rangle \approx 0.0065$ $(eV)^2$ calculated for the reference structure.[71] In addition, clusters A, B, C, and D, have twist angle between 9° and 27°. These values are smaller than the twist angle 36° reported for the ideal π stack of B-DNA,[75,76] but are close to the twist of 17−20° found for PNA.[77,78] Table 1 also shows that for structures with the similar twist angles, V^2_{cl} (as expected) decreases as translations become larger (*cf.* the results for clusters A and D). The configurations

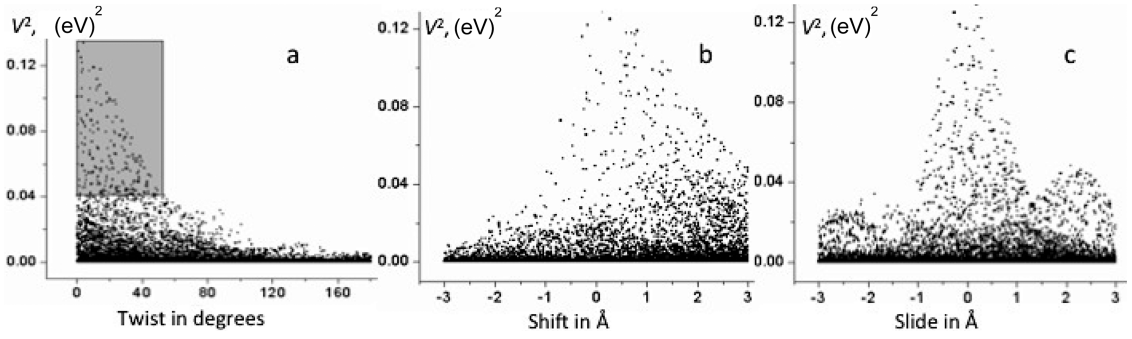

Figure 3. Scatter plot of the electronic coupling squared V^2 *vs* the values of twist (a), shift (b), and slide (c).

TABLE 1. Results of the Cluster Analysis Performed for 6097 Conformations of the [(G:C),(G:C)] Dimer with Twist ≤50°. The Data Refer Only to Clusters with Electronic Coupling Squared ≥0.030 (eV)²

clusters	number of points	V_{cl}^2, (eV)²	shift, Å	slide, Å	twist, degrees
A	98	0.099 ± 0.015	0.55 ± 0.54	0.06 ± 0.32	9.9 ± 7.1
B	190	0.065 ± 0.010	1.19 ± 0.74	0.13 ± 0.49	22.1 ± 9.1
C	184	0.032 ± 0.008	2.26 ± 0.56	2.14 ± 0.56	26.7 ± 6.9
D	254	0.031 ± 0.008	1.01 ± 0.82	1.31 ± 0.95	9.4 ± 6.1

corresponding to cluster centroids are depicted in Figure 4.

Highly Conductive [(A:T),(A:T)] Dimer Structures. A computational search for structures with high conductance was also performed for the [(A:T),(A:T)] dimer. The results of the cluster analysis obtained for the dimer conformations with the twist angle ≤50° are summarized in Table 2. As can be seen, the V_{cl}^2 values for highly conductive structures belonging to clusters A, B, C, and D exceed at least by 1 order of magnitude the value of electronic coupling 0.003 (eV)² obtained for the reference structure.[79] Similar to [(G:C),(G:C)] duplexes, the configurations of the [(A:T),(A:T)] dimer with the largest value of V_{cl}^2 (clusters A and B) have relatively small twist, less than 36° found for the ideal π stack of B-DNA (see *e.g.,* refs 59 and 68). Note that like the [(G:C),(G:C)] duplexes, the [(A:T),(A:T)] dimers exhibit relatively large electronic coupling squared and hence high hopping conductance in the cases of configurations with significant translations of base pairs (cluster D) or with the twist ~36° (cluster C).

In addition, the results presented in Table 2 show that there are configurations exhibiting high conductance with significant translations of base pairs (cluster C). Note that unlike the [(G:C),(G:C)] duplexes, the [(A:T),(A:T)] dimers exhibit relatively large electronic coupling in configurations with the twist ~36° (cluster C).

It is interesting that according to the cluster analysis, the most conductive conformations of [(A:T),(A:T)] and [(G:C),(G:C)] dimers have similar V_{cl}^2 values (*cf.* the data for clusters A in Tables 1 and 2). This enables one to assume that the difference in the zero bias hopping conductance along poly(A)−poly(T) and poly(G)−poly(C)

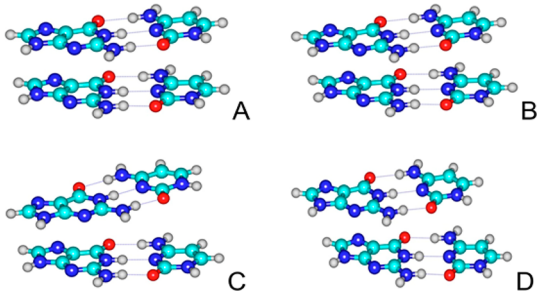

Figure 4. Arrangement of two neighboring G:C base pairs in dimers with structural parameters corresponding to centroids of clusters A, B, C, and D (see Table 1). Atoms H, C, N, and O are shown in gray, cyan, blue, and red, respectively. Three hydrogen bonds between G and C are also depicted.

TABLE 2. Results of the Cluster Analysis Performed for [(A:T),(A:T)] Dimer Conformations with Twist ≤50°. The Data Refer Only to Clusters with Electronic Coupling Squared ≥0.030 (eV)²

clusters	number of points	V_{cl}^2, (eV)²	shift, Å	slide, Å	twist, degrees
A	85	0.121 ± 0.018	0.44 ± 0.43	0.07 ± 0.34	10.1 ± 7.3
B	203	0.072 ± 0.015	0.72 ± 0.68	0.19 ± 0.62	17.1 ± 8.9
C	168	0.044 ± 0.010	1.80 ± 0.77	0.95 ± 0.96	35.9 ± 7.2
D	248	0.032 ± 0.009	1.84 ± 0.74	1.84 ± 0.66	12.0 ± 6.9

stacks is mainly due to the higher position of the HOMO level for G than for A bases, rather than to the distinct values of their electronic coupling. Recent experimental data on the HOMO energy gap dependence of hole transfer kinetics in DNA[56] strongly support this assumption.

Corrections for Thermal Fluctuations. Although the cluster analysis suggests structural regions where electronic coupling for [(A:T),(A:T)] and [(G:C),(G:C)] dimers is larger than for corresponding reference structures, our estimates can be quite crude because they neglect the effect of thermal fluctuations on the values of the step and base pair parameters. In particular, it was assumed that base pairs in the stack have strictly planar arrangement, with both tilt and roll angles taken to be zero for all configurations. In addition, the rise parameter was assumed to remain unchanged.

To obtain more reliable estimates, any step parameter p_i was considered as a real-valued random variable clustered around a single mean value $\bar{p}_i$ in accordance with the normal (Gaussian) distribution

$$w(p_i) = \frac{1}{\sqrt{2\pi\sigma_{p_i}^2}} \exp\left[-\frac{(p_i - \bar{p}_i)^2}{2\sigma_{p_i}^2}\right] \quad (4)$$

where $\sigma_{p_i}^2$ is the variance characterizing the structural flexibility of the π stack and $i = 1, 2, 3, 4, 5$, and 6 for shift, slide, twist, tilt, roll, and rise, respectively. The mean values for shift, slide, and twist were taken from the results of cluster analysis (see Tables 1 and 2). Parameters tilt and roll ($\bar{p}_4$ and $\bar{p}_5$) were set to be zero, while for rise, $\bar{p}_6$ was equal to 3.4 Å. To generate stack conformations, the following values of the variance $\sigma_{p_i}^2$ were assumed: $\sigma_{p_1}^2 = \sigma_{p_2}^2 = 0.5$ Å^2 for shift and slide, $\sigma_{p_6}^2 = 0.3$ Å^2 for rise, and $\sigma_{p_3}^2 = \sigma_{p_4}^2 = \sigma_{p_5}^2 = 5$ grad^2 for twist, tilt, and roll. These values are close to the standard deviations of the step parameters extracted from the analysis of A and B-DNA crystal structures[76] and MD simulations.[80]

Some structures generated with this scheme may have unreasonably short van der Waals contact distances, d_{VdW}, between atoms belonging to distinct base pairs. To find such configurations, we compute the energy, E, of the electrostatic and van der Waals interactions of base pairs in the duplexes[81] using the Amber 95 force field.[82] The results of these calculations were then compared with the interaction energy, $\bar{E}$, found for the reference structure determined by the step parameters $\{\bar{p}_i\}$ in eq 4. Since the difference between these two quantities cannot be larger than the interaction energy of base pairs in dimers (about 5 kcal/mol[83]), all conformations with $E > \bar{E} + 5$ kcal/mol should be excluded from consideration as structures with far too small d_{VdW} values.

The computational approach described above enables one to model the impact of thermal fluctuations on the electronic coupling. The effective value V_{eff}^2 was obtained by averaging V^2 over one thousand structures allowed from the standpoint of energy.

The values of V_{eff}^2 calculated for [(A:T),(A:T)] and [(G:C),(G:C)] dimers by taking into account thermal fluctuations in these duplexes are given in Table 3. The electronic coupling squared, V_1^2, estimated for a single dimer configuration with the step parameters given in Tables 1 and 2, together with the value of this quantity V_{cl}^2 predicted by the *k*-means clustering method are also presented in this Table.

Comparison of the data shown in Table 3 demonstrates that in clusters B, C, and D for both dimers, the obtained V_{cl}^2 and V_{eff}^2 values are close to each other. Generally, the V_1^2 values computed for a single structures corresponding to the centroid of the cluster can deviate considerably from the effective coupling as found for cluster D of [(G:C),(G:C)]. This is because of the high sensitivity of electronic coupling to structural

TABLE 3. Electronic Couplings Squared (in (eV)^2) Computed for [(G:C),(G:C)] and [(A:T),(A:T)] Stacked Dimers

[(G:C),(G:C)] dimer duplex				[(A:T),(A:T)] dimer duplex			
clusters	V_1^2	V_{cl}^2	V_{eff}^2	clusters	V_1^2	V_{cl}^2	V_{eff}^2
A	0.128	0.099	0.072	A	0.152	0.121	0.086
B	0.104	0.065	0.062	B	0.133	0.072	0.077
C	0.043	0.032	0.033	C	0.036	0.044	0.031
D	0.59×10^{-4}	0.031	0.020	D	0.042	0.032	0.034

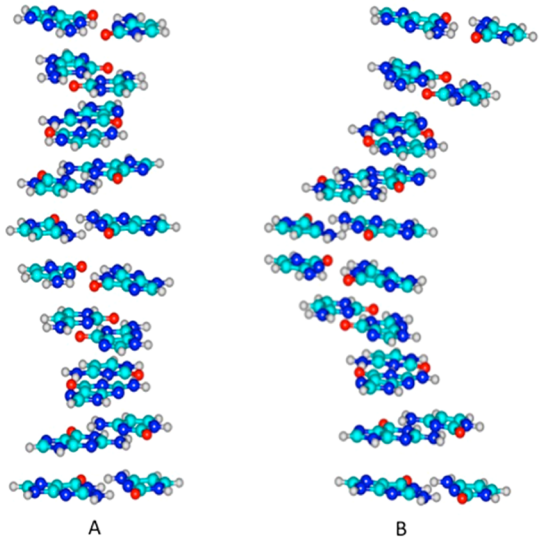

Figure 5. Structures of the reference B-DNA oligomer containing 10 stacked G:C base pairs (A) and poly(G)−poly(C) sequence (B) with enhanced conductance compared to (A). The poly(G)−poly(C) sequence has the same values of step parameters as those found for cluster C in Table 1. Atoms H, C, N, and O are shown in gray, cyan, blue, and red, respectively.

parameters. In most cases, however, we found that V_1^2 is close to the largest value of electronic coupling computed in the conformational space of the cluster. Averaging over all configurations leads to a decrease of the coupling ($V_{cl}^2 < V_1^2$) because of including structures with smaller values of V^2. Thermal fluctuations may lead to a further decrease of the coupling, so that V_{eff}^2 can become smaller than V_{cl}^2 mainly due to the inclusion of configurations with a nonparallel arrangement of the base pairs. The latter effect is evident for cluster A with the strongest coupling as well as for cluster D of [(G:C),(G:C)] For other clusters, the distinction between the values of V_{eff}^2 and V_{cl}^2 almost vanishes. This implies that additional conformations with nonparallel alignment of adjacent base pairs, which are involved in averaging, do not significantly change V^2. Therefore the mean effect of thermal fluctuations is properly described by the structures forming the cluster.

Structure of Homogeneous Sequences with Enhanced Hopping Conductance. Once the configurations of [(G:C),(G:C)] and [(A:T),(A:T)] dimer duplexes with $\langle V^2 \rangle$ exceeding

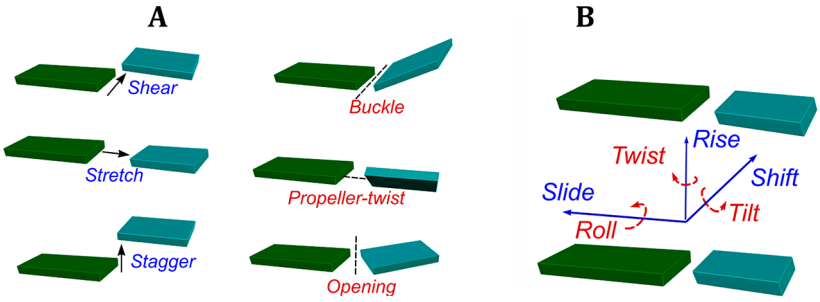

Figure 6. Base pair (A) and step (B) parameters used to define π-stack geometries. Parameters describing translations and rotations are shown in blue and red, respectively.

the reference values have been identified, one can computationally construct structures of the entire poly(G)−poly(C) and poly(A)−poly(T) stacks with improved conducting properties, using for this purpose the program X3DNA[84] and the step parameters listed in Table 1 and Table 2.

Atomic coordinates for four duplexes $(GC)_{10}$ and four duplexes $(AT)_{10}$ are given in the Supporting Information. The example of such a representative construct together with the reference structure of the B-DNA oligomer containing 10 G:C base pairs are shown in Figure 5. It is interesting to compare the zero-bias hopping conductance g for two structures represented in this figure. For 10-mer B-DNA reference system, g can be evaluated using eq 1 with k_{CT} obtained from the experimental data on the hole arrival rate in the G tract.[55] This evaluation yields $g \approx 1$ nS. Since the charge transfer rate linearly scales with the mean electronic coupling squared, which has already been calculated for poly(G)−poly(C) depicted in Figure 5B (see the data for cluster C in Table 1), we find that g for this stack is 7 nS. Thus, we infer that in the regime of sequential hopping the poly(G)−poly(C) stack with structure shown in Figure 5 B is seven times more conductive than the reference B-DNA oligomer with 10 stacked G:C pairs. Greater improvement of hopping conductance should be expected for the poly(G)−poly(C) stack constructed exploiting the configuration of cluster A in Table 1. In the latter case the hopping conductance along homogeneous poly(G)−poly(C) sequence is 15 times as large as the conductance of the B-DNA oligomer in Figure 5A.

The values of parameters found for the dimers appears to be appropriate for computational construction of longer DNA sequences as soon as sequential hopping remains the main mechanism of hole transport through homogeneous DNA oligonucleotides. In this case the electronic interaction with flanking pairs does not change significantly the coupling of neighboring base pairs. Because of these reasons, the values of parameters employed in the computational construction of the [(G:C),(G:C)] dimer duplex and DNA oligomer shown in Figure 5B were taken to be the same.

The question now arises whether the configurations of conducting stacks predicted by our calculations can be realized in the lab. Although the answer to this question is beyond the scope of the present work, several possibilities that can be used to make desirable changes in the values of step parameters for base pair stacks in DNA are worthy of brief consideration here. These include the following:

(1) *Chemical modification of DNA backbone.* A typical example is the substitution of the phosphoribose backbone of DNA with a pseudopeptide consisting of *N*-(2-aminoethyl)-glycine units with a methylene carbonyl linker connecting to the nucleobase. Such a substitution affects the conformation of the base pair stack, reducing the average twist angle to 19.8°.[78,85,86] As a consequence, the base pair stack adopts the configuration that is close to the configuration of clusters A, B, and D in Table 1. Another example is an "all LNA" duplex containing exclusively modified β-D-2′-*O*-4′C-methylene ribofuranose nucleotides.[87] In this case the twist angle is equal to 26° instead of 36° as known for B-DNA, rise becomes 2.8 Å as compared to 3.4 Å for B-DNA. In addition, depending on degree of the LNA modification of the 9-mer duplexes the absolute values of shift and slide parameters vary from 0.1 Å up to 0.6 Å and from 0.5 Å up to 2.0 Å, respectively.[88] Since for clusters listed in Table 1, shift was found to be in the ranges between 0.7 Å and 2.1 Å while slide falls in the range from 0.1 Å to 1.9 Å, it can be expected that the proper LNA modification will allow base pair stacks to have conformations similar to those deduced computationally.

(ii) *Solvent-induced changes in conformations of base pair stack.* To alter the values of step parameters in the stack of base pairs inside DNA one also can increase the water content around and inside the double helix. This induces a transition from the A-form to the B-form of DNA accompanied by the decrease of helical twist and the magnitude of the base pair slide.[89] It should be mentioned that the A to B transition occurs through a set of intermediate conformations with different values of twist and rise parameters. Methylation and bromination of cytosine allow each of these intermediates to be trapped in their particular configuration.

(iii) *Changes of step parameters in the presence of ions.* Ions have a significant impact on the conformation of DNA molecule and hence on the values of step

parameters of the base pair stack (see e.g., ref 90 and references therein). In particular, investigations of the 1.6-Å X-ray structure of the Dickerson–Drew dodecamer composed of $[d(CGCGAAXXCGCG]_2$ with X being effectively a thymine residue linked at the 5 positions to an *n*-propyl-amine have clearly demonstrated the effect of the tethered positive charge on the conformation of the base pair stack.[91] It has been shown that the tethered cations directed in the 3′ direction, toward a phosphate group near one end of a duplex induce changes in the values of rise, twist, and roll parameters.

(iv) *Impact of external mechanical forces on geometry of base pair stack.* It is well-known that external mechanical forces are able to affect the arrangement of stacked base pairs (see *e.g.*, refs 92 and 93 and references therein). The forced extension of DNA leads to the transition of this biomolecule from classical B-form to the so-called S-form, which is almost completely unwound and contains base pairs tilted with respect to the helix axis. This form of DNA can be transformed into a zipper-like (zip-) structure,[93] though the formation of a denaturation bubble inside the double helix is also possible as soon as double stranded DNA is sufficiently extended.[92] Note that in zip-DNA the bases of the DNA strands interdigitate with each other and form a single-base aromatic stack, thus increasing electronic coupling and zero-biased conductance of the DNA structure.[89]

Thus, the ability of DNA to adopt a number of helical forms depending on the external conditions, applied mechanical forces, and chemical modification of the backbone, offers possibilities to vary the arrangement of base pairs stacked inside the double helix. Furthermore, each of the above-mentioned factors alone or in combination with other factors causes changes in the values of step parameters favorable to the formation of the stack conformation, providing high conductance of DNA molecules.

SUMMARY AND CONCLUSIONS

On the basis of the combination of the computationally efficient and quite accurate method for quantum mechanical calculations of the electronic coupling and the *k*-means clustering data analysis technique, we developed a methodology for searching the region of DNA step parameters and DNA structures with large electronic coupling and hence with high zero-bias intramolecular hopping conductance. Our results clearly show that a remarkable increase in conductance of base pair stacks can be achieved using a relatively small number of conformations with structures exhibiting the strongest electronic coupling. Using the proposed computational methodology, we demonstrate the possibility to identify structures of homogeneous poly(A)–poly(T) and poly(G)–poly(C) stacks with zero-bias intramolecular hopping conductance significantly larger (by ratios up to 15) than the value of this important physical quantity found for conventional B-DNA. To verify the reliability of our estimates, the impact of thermal fluctuations on the averaged dimer structures deduced from the cluster analysis was modeled. The results show that thermal fluctuations do not substantially change the values of electronic coupling squared calculated for configurations identified by the cluster analysis.

Certainly we recognize that other parameters, especially the reorganization energy, are extremely important for exploring hole transport through DNA. However one cannot ignore the contribution of electronic coupling in the conductance as well. Furthermore it is possible to separate the two effects mentioned above. In the submitted manuscript we are focused on electronic coupling in structurally very different stacks. The matrix element characterizing this coupling is known to be rather insensitive to the external electric field of surroundings. Owing to the latter circumstance the results obtained are applicable both to the gas and to the condensed media. The environment effects are mainly determined by the backbone (*e.g.*, whether it carries a net charge as in DNA or not as in PNA), the polarity, and dynamics of solvent molecules around DNA. This aspect of the problem deserves a separate investigation since it lies beyond the scope of the present study.

COMPUTATIONAL METHODOLOGY

Model Structures. To measure molecular conductance under conditions similar to those of real devices, DNA oligomers should have lengths comparable to or larger than a sub-10-nm gap between two metallic electrodes.[94] As discussed above, on such distance scales hole transport and DNA molecular conductance should proceed mainly *via* multistep sequential hopping. Moreover, for the most conductive homogeneous poly(A)–poly(T) and poly(G)–poly(C) stacks the elementary motion step always represents a process involving two neighboring either A:T or G:C base pairs. For this reason, we consider only fragments of the DNA structure involving dimer duplexes [(G:C),(G:C)] and [(A:T),(A:T)] as the model assemblies.

The structural parameters characterizing individual base pairs that form the dimer duplexes under consideration are schematically shown in Figure 6A. These parameters can be separated into two main groups, that is, translations (shear, stretch, and stagger) and rotations (buckle, propeller-twist, and opening). As follows from Figure 6B, the same two groups are exploited to describe base pair steps. In the latter case, however, translations include slide, shift, and rise, while rotations involve tilt, roll, and twist.

Detailed discussion of the base pair and step parameters can be found elsewhere.[75,76] The search for base pair stack structures that provide high conductance in DNA imposes certain limitations on the values of these parameters. In particular, the six structural parameters shown in Figure 6A (shear, stretch, stagger, buckle, propeller-twist, and opening) should be zero, because electronic coupling between components of [(G:C),(G:C)] and [(A:T),(A:T)] dimers and hence the electric conductance of homogeneous stacks poly(G)-poly(C) and poly(A)-poly(T) have the largest values for parallel arrangements of base pairs.[57] For the same

reason, roll and tilt were taken to be 0°. The values of shift and slide parameters were randomly generated within the interval from −3.0 Å to +3.0 Å. As follows from the comparison of these two boundary values with the values of base-pair parameters reported for B- and A-DNA crystal structures at high resolution,[76] independent variation of shift and slide in the range from −3.0 to +3.0 Å will cover all possible horizontal translations of base pairs in stable π stacks. The value of the twist angle was also chosen randomly to vary from 0° to 180°. It should be noted that any two DNA π-stacks generated with the program X3DNA[84] using parameters (shift, slide, rise, tilt, roll, twist) and (−shift, slide, rise, tilt, −roll, −twist) are structurally identical. So consideration of structures with negative twist would be redundant. In all preliminary calculations associated with the scanning of the conformational space, the rise parameter had the same value 3.4 Å as in B-form DNA.[95−97]

Large variations of the selected parameters (twist, shift, and slide) may be justified by taking into account that to ensure the effective π stacking of two neighboring base pairs, their planes should be parallel. Furthermore, in most organic π stacks rise = 3.4 ± 0.3 Å, so that the value of this parameter does not change much. Moreover, the coupling varies with rise as $\exp(-\gamma \cdot \text{rise})$. This implies that for any configuration rise should be as small as possible. As regards to tilt and roll, usually these parameters are close to zero; otherwise the planes of base pairs will never be parallel. It should be emphasized that thermal fluctuations of these three parameters are taken into account by calculating the final values of the coupling.

Atomic coordinates of the stacks were calculated using the program X3DNA.[84]

By varying shift, slide, and twist 22 000 configurations with parallel base pair planes were generated for each dimer duplex. These configurations were used to calculate electron coupling for hole transfer between base pairs in [(G:C),(G:C)] and [(A:T),(A:T)] model duplexes as explained below.

Calculations of Electronic Coupling. According to the fragment charge difference (FCD) method,[98] the electronic coupling matrix element V between the donor site D and the acceptor site A can be written as

$$V = \frac{(E_2 - E_1)|\Delta q_{12}|}{\sqrt{(\Delta q_1 - \Delta q_2)^2 + 4\Delta q_{12}^2}} \quad (5)$$

Here Δq_1 and Δq_2 are the donor−acceptor charge differences in the adiabatic states with energies E_1 and E_2, and Δq_{12} is the corresponding off-diagonal term. These quantities were calculated within the self-consistent field approximation using the semiempirical INDO/S method[68] as described in detail elsewhere.[98] The method was shown to be computationally very efficient, offering surprisingly good estimates for electronic couplings in DNA stacks.[99] These advantages enable quantum mechanical treatment of several thousand different conformations of stacked base pairs.

Data Analysis. To analyze the results of our computational studies, n data points ($\mathbf{x}_1$, $\mathbf{x}_2$, ..., $\mathbf{x}_n$) obtained for each investigated duplex were represented as a set of 4-dimensional real vectors. These vectors are defined by their components that include electronic coupling squared, V^2, and three step parameters (shift, slide, and twist) characterizing the structure of a system. In the context of the present investigation the data analysis is aimed at finding the regions for values of step parameters where the dimer structure ensures large couplings and therefore high electric conductance.

To achieve this objective we used the method of data analysis called k-means clustering that allows partitioning of n data points into the set $\mathbf{S} = \{S_1, S_2, ..., S_k\}$ of k clusters ($k \leq n$).[69,70] Usually the grouping is accomplished by minimizing the within-cluster sum of squares:

$$\arg\min_{S} \sum_{i=1}^{k} \sum_{x_j \in S_i} || x_j - \mu_i ||^2 \quad (6)$$

where μ_i is the mean of points in S_i. As a result, vectors in the same cluster are very similar in values of their components as opposed to vectors belonging to different clusters. The latter have components that dramatically differ in magnitude.

Computationally the cluster analysis was realized using the program Tanagra.[74] This program enables one to find clusters with shift, slide, and twist that define structures of dimer duplexes with V^2 and g far beyond the values of these parameters calculated for analogous reference systems. The reference systems correspond to two neighboring base pairs in poly(G)−poly(C) and poly(A)−poly(T) sequences of B-DNA in solution. For these reference structures, the average electronic coupling squared, V^2, was computed to be 0.01 $(\text{eV})^2$ and 0.003 $(\text{eV})^2$ for [(G:C),(G:C)] and [(A:T),(A:T)] dimers, respectively.[71,79]

Conflict of Interest: The authors declare no competing financial interest.

Acknowledgment. This publication is based upon investigations supported by the Department of the Navy, Office of Naval Research, under Award N00014-11-1-0729. Y. Berlin and M. Ratner are grateful to DoD/MURI and the Office of Naval Research for the financial support of their work. A. Voityuk thanks Ministry of Science and Innovation, Spain and the FEDER fund for their financial support under Grants CTQ 2011-26573, UNGI08-4E-003 and UNGI10-4E-801.

Supporting Information Available: Atomic coordinates of π stacked $(GC)_{10}$ and $(AT)_{10}$ structures with step parameters listed in Tables 1 and 2, respectively (structures are provided in the PDB (Protein Data Base) format). This material is available free of charge *via* the Internet at http://pubs.acs.org.

REFERENCES AND NOTES

1. Seeman, N. C. Nanomaterials Based on DNA. In *Annual Review of Biochemistry*; Kornberg, R. D., Raetz, C. R. H., Rothman, J. E., Thorner, J. W., Eds.; 2010; Vol. *79*, pp 65−87.
2. Cutler, J. I.; Auyeung, E.; Mirkin, C. A. Spherical Nucleic Acids. *J. Am. Chem. Soc.* **2012**, *134*, 1376–1391.
3. Shin, J. S.; Pierce, N. A. A Synthetic DNA Walker for Molecular Transport. *J. Am. Chem. Soc.* **2004**, *126*, 10834–10835.
4. Sherman, W. B.; Seeman, N. C. A Precisely Controlled DNA Biped Walking Device. *Nano Lett.* **2004**, *4*, 1203–1207.
5. Omabegho, T.; Sha, R.; Seeman, N. C. A Bipedal DNA Brownian Motor with Coordinated Legs. *Science* **2009**, *324*, 67–71.
6. Porath, D.; Bezryadin, A.; de Vries, S.; Dekker, C. Direct Measurement of Electrical Transport through DNA Molecules. *Nature* **2000**, *403*, 635–638.
7. Cohen, H.; Nogues, C.; Naaman, R.; Porath, D. Direct Measurement of Electrical Transport through Single DNA Molecules of Complex Sequence. *Proc. Natl. Acad. Sci. U.S. A.* **2005**, *102*, 11589–11593.
8. Xu, B.; Zhang, P.; Li, X.; Tao, N. J. Direct Conduction Measurement of Single DNA Molecules in Aqueous Solution. *Nano Lett* **2004**, *4*, 1105–1108.
9. Hihath, J.; Xu, B. Q.; Zhang, P. M.; Tao, N. J. Study of Single-Nucleotide Polymorphisms by Means of Electrical Conductance Measurements. *Proc. Natl. Acad. Sci. U.S.A.* **2005**, *102*, 16979–16983.
10. Nunez, M. E.; Hall, D. B.; Barton, J. K. Long-Range Oxidative Damage to DNA: Effects of Distance and Sequence. *Chem. Biol.* **1999**, *6*, 85–97.
11. Williams, T. T.; Odom, D. T.; Barton, J. K. Variations in DNA Charge Transport with Nucleotide Composition and Sequence. *J. Am. Chem. Soc.* **2000**, *122*, 9048–9049.
12. Henderson, P. T.; Jones, D.; Hampikian, G.; Kan, Y. Z.; Schuster, G. B. Long-Distance Charge Transport in Duplex DNA: The Phonon-Assisted Polaron-like Hopping Mechanism. *Proc. Natl. Acad. Sci. U.S.A.* **1999**, *96*, 8353–8358.
13. Sanii, L.; Schuster, G. B. Long-Distance Charge Transport in DNA: Sequence-Dependent Radical Cation Injection Efficiency. *J. Am. Chem. Soc.* **2000**, *122*, 11545–11546.
14. Schuster, G. B. Long-Range Charge Transfer in DNA: Transient Structural Distortions Control the Distance Dependence. *Acc. Chem. Res.* **2000**, *33*, 253–260.
15. Meggers, E.; Michel-Beyerle, M. E.; Giese, B. Sequence Dependent Long Range Hole Transport in DNA. *J. Am. Chem. Soc.* **1998**, *120*, 12950–12955.

16. Giese, B.; Wessely, S.; Spormann, M.; Lindemann, U.; Meggers, E.; Michel-Beyerle, M. E. On the Mechanism of Long-Range Electron Transfer through DNA. *Angew. Chem., Int. Ed.* **1999**, *38*, 996–998.
17. Giese, B.; Wessely, S. The Influence of Mismatches on Long-Distance Charge Transport through DNA. *Angew. Chem., Int. Ed.* **2000**, *39*, 3490–3491.
18. Giese, B. Long Distance Charge Transport in DNA: The Hopping Mechanism. *Acc. Chem. Res.* **2000**, *33*, 631–636.
19. Giese, B.; Amaudrut, J.; Kohler, A. K.; Spormann, M.; Wessely, S. Direct Observation of Hole Transfer through DNA by Hopping between Adenine Bases and by Tunnelling. *Nature* **2001**, *412*, 318–320.
20. Dekker, C.; Ratner, M. A. Electronic Properties of DNA. *Phys. World* **2001**, *14*, 29–33.
21. Di Ventra, M.; Zwolak, M. DNA Electronics. In *Encyclopedia of Nanoscience and Nanotechnology*; Nalwa, H. S., Ed.; American Scientific Publishers: New York, 2004; Vol. 2, pp 475–493.
22. Schuster, G. B. *Long-Range Charge Transfer in DNA I*; Springer-Verlag: Berlin, 2004; Vol. 236.
23. Schuster, G. B. *Long-Range Charge Transfer in DNA II*; Springer-Verlag: Berlin, 2004; Vol. 237.
24. Chakraborty, T. *Charge Migration in DNA. Prospectives from Physics, Chemistry, and Biology*; Springer-Verlag: Berlin, 2007.
25. Wagenknecht, H.-A. *Charge Transfer in DNA: From Mechanism to Application*; Wiley-VCH Verlag GmbH & Co KGaA: Weinheim. Germany, 2005.
26. Bixon, M.; Giese, B.; Wessely, S.; Langenbacher, T.; Michel-Beyerle, M. E.; Jortner, J. Long-Rang Charge Hopping in DNA. *Proc. Natl. Acad. Sci. U.S.A* **1999**, *96*, 11713–11716.
27. Grozema, F. C.; Berlin, Y. A.; Siebbeles, L. D. A. Sequence-Dependent Charge Transfer in Donor–DNA–Acceptor Systems: A Theoretical Study. *Int. J. Quantum Chem.* **1999**, *75*, 1009–1016.
28. Berlin, Y. A.; Burin, A. L.; Ratner, M. A. On the Long-Range Charge Transfer in DNA. *J. Phys. Chem. A* **2000**, *104*, 443–445.
29. Grozema, F. C.; Berlin, Y. A.; Siebbeles, L. D. A. Mechanism of Charge Migration through DNA: Molecular Wire Behavior, Single-Step Tunneling or Hopping? *J. Am. Chem. Soc.* **2000**, *122*, 10903–10909.
30. Berlin, Y. A.; Burin, A. L.; Ratner, M. A. Charge Hopping in DNA. *J. Am. Chem. Soc.* **2001**, *123*, 260–268.
31. Seidel, C. A. M.; Schulz, A.; Sauer, M. H. M. Nucleobase-Specific Quenching of Fluorescent Dyes. 1. Nucleobase One-Electron Redox Potentials and Their Correlation with Static and Dynamic Quenching Efficiencies. *J. Phys. Chem.* **1996**, *100*, 5541–5553.
32. Steenken, S.; Jovanovic, S. V. How Easily Oxidizable Is DNA? One-Electron Reduction Potentials of Adenosine and Guanosine Radicals in Aqueous Solution. *J. Am. Chem. Soc.* **1997**, *119*, 617–618.
33. Voityuk, A. A.; Jortner, J.; Bixon, M.; Rösch, N. Energetics of Hole Transfer in DNA. *Chem. Phys. Lett.* **2000**, *324*, 430–434.
34. Berlin, Y. A.; Burin, A. L.; Ratner, M. A. Elementary Steps for Charge Transport in DNA: Thermal Activation *vs.* Tunneling. *Chem. Phys.* **2002**, *275*, 61–74.
35. Bixon, M.; Jortner, J. Long-Range and Very Long-Range Charge Transport in DNA. *Chem. Phys.* **2002**, *281*, 393–408.
36. Lewis, F. D.; Zhu, H. H.; Daublain, P.; Cohen, B.; Wasielewski, M. R. Hole Mobility in DNA a Tracts. *Angew. Chem., Int. Ed.* **2006**, *45*, 7982–7985.
37. Lewis, F. D.; Zhu, H. H.; Daublain, P.; Fiebig, T.; Raytchev, M.; Wang, Q.; Shafirovich, V. Crossover from Superexchange to Hopping as the Mechanism for Photoinduced Charge Transfer in DNA Hairpin Conjugates. *J. Am. Chem. Soc.* **2006**, *128*, 791–800.
38. Choi, S. H.; Kim, B.; Frisbie, C. D. Electrical Resistance of Long Conjugated Molecular Wires. *Science* **2008**, *320*, 1482–1486.
39. Lu, Q.; Liu, K.; Zhang, H. M.; Du, Z. B.; Wang, X. H.; Wang, F. S. From Tunneling to Hopping: A Comprehensive Investigation of Charge Transport Mechanism in Molecular Junctions Based on Oligo(P-Phenylene Ethynylene)S. *ACS Nano* **2009**, *3*, 3861–3868.
40. Hines, T.; Diez-Perez, I.; Hihath, J.; Liu, H. M.; Wang, Z. S.; Zhao, J. W.; Zhou, G.; Muellen, K.; Tao, N. J. Transition from Tunneling to Hopping in Single Molecular Junctions by Measuring Length and Temperature Dependence. *J. Am. Chem. Soc.* **2010**, *132*, 11658–11664.
41. Choi, S. H.; Risko, C.; Delgado, M. C. R.; Kim, B.; Bredas, J. L.; Frisbie, C. D. Transition from Tunneling to Hopping Transport in Long, Conjugated Oligo-Imine Wires Connected to Metals. *J. Am. Chem. Soc.* **2010**, *132*, 4358–4368.
42. Luo, L.; Choi, S. H.; Frisbie, C. D. Probing Hopping Conduction in Conjugated Molecular Wires Connected to Metal Electrodes. *Chem. Mater.* **2011**, *23*, 631–645.
43. Segal, D.; Nitzan, A.; Davis, W. B.; Wasielewski, M. R.; Ratner, M. A. Electron Transfer Rates in Bridged Molecular Systems 2. A Steady-State Analysis of Coherent Tunneling and Thermal Transitions. *J. Phys. Chem. B* **2000**, *104*, 3817–3829.
44. Nitzan, A. A Relation between Electron Transfer Rate and Molecular Conductance. *J. Phys. Chem. A* **2001**, *105*, 2677–2679.
45. Nitzan, A.; Ratner, M. A. Electron Transport in Molecular Wire Junctions. *Science* **2003**, *300*, 1384–1389.
46. Nitzan, A. The Relation between Electron Transfer Rate and Molecular Conduction. 2. The Sequential Hopping Case. *Isr. J. Chem.* **2002**, *42*, 163–166.
47. Bixon, M.; Jortner, J. Incoherent Charge Hopping and Conduction in DNA and Long Molecular Chains. *Chem. Phys.* **2005**, *319*, 273–282.
48. Berlin, Y. A.; Ratner, M. A. Intra-molecular Electron Transfer and Electric Conductance *via* Sequential Hopping: Unified Theoretical Description. *Radiat. Phys. Chem.* **2005**, *74*, 124–131.
49. Giese, B.; Meggers, E.; Wessely, S.; Spormann, M.; Biland, A. DNA as a Supramolecule for Long-Distance Charge Transport. *Chimia* **2000**, *54*, 547–551.
50. Shao, F. W.; Augustyn, K.; Barton, J. K. Sequence Dependence of Charge Transport through DNA Domains. *J. Am. Chem. Soc.* **2005**, *127*, 17445–17452.
51. Takada, T.; Kawai, K.; Fujitsuka, M.; Majima, T. Contributions of the Distance-Dependent Reorganization Energy and Proton-Transfer to the Hole-Transfer Process in DNA. *Chem.—Eur. J.* **2005**, *11*, 3835–3842.
52. Lewis, F. D.; Zuo, X.; Liu, J.; Hayes, R. T.; Wasielewski, M. R. Dynamics of Inter- and Intrastrand Hole Transport in DNA Hairpins. *J. Am. Chem. Soc.* **2002**, *124*, 4568–4569.
53. Lewis, F. D.; Liu, J.; Zuo, X.; Hayes, R. T.; Wasielewski, M. R. Dynamics and Energetics of Single-Step Hole Transport in DNA Hairpins. *J. Am. Chem. Soc.* **2003**, *125*, 4850–4861.
54. Senthilkumar, K.; Grozema, F. C.; Guerra, C. F.; Bickelhaupt, F. M.; Lewis, F. D.; Berlin, Y. A.; Ratner, M. A.; Siebbeles, L. D. A. Absolute Rates of Hole Transfer in DNA. *J. Am. Chem. Soc.* **2005**, *127*, 14894–14903.
55. Conron, S. M. M.; Thazhathveetil, A. K.; Wasielewski, M. R.; Burin, A. L.; Lewis, F. D. Direct Measurement of the Dynamics of Hole Hopping in Extended DNA G-Tracts. An Unbiased Random Walk. *J. Am. Chem. Soc.* **2010**, *132*, 14388–14390.
56. Kawai, K.; Hayashi, M.; Majima, T. HOMO Energy Gap Dependence of Hole Transfer Kinetics in DNA. *J. Am. Chem. Soc.* **2012**, *134*, 4806–4811.
57. Voityuk, A. A.; Siriwong, K.; Rösch, N. Charge Transfer in DNA. Sensitivity of Electronic Couplings to Conformational Changes. *Phys. Chem. Chem. Phys.* **2001**, *3*, 5421–5425.
58. Grozema, F. C.; Tonzani, S.; Berlin, Y. A.; Schatz, G. C.; Siebbeles, L. D. A.; Ratner, M. A. Effect of Structural Dynamics on Charge Transfer in DNA Hairpins. *J. Am. Chem. Soc.* **2008**, *130*, 5157–5166.
59. Siriwong, K.; Voityuk, A. A. π Stack Structure and Hole Transfer Couplings in DNA Hairpins and DNA. A Combined QM/MD Study. *J. Phys. Chem. B* **2008**, *112*, 8181–8187.
60. Kubar, T.; Elstner, M. What Governs the Charge Transfer in DNA? The Role of DNA Conformation and Environment. *J. Phys. Chem. B* **2008**, *112*, 8788–8798.

61. Gutierrez, R.; Caetano, R. A.; Woiczikowski, B. P.; Kubar, T.; Elsner, M.; Cuniberti, G. Charge Transport through Biomolecular Wire in a Solvent: Bridging Molecular Dynamics and Model Hamiltonian Approaches. *Phys. Rev. Lett.* **2009**, *102*, 208102.
62. Gutierrez, R.; Caetano, R.; Woiczikowski, P. B.; Kubar, T.; Elstner, M.; Cuniberti, G. Structural Fluctuations and Quantum Transport through DNA Molecular Wires: A Combined Molecular Dynamics and Model Hamiltonian Approach. *New J. Phys.* **2010**, *12*, 023022.
63. Bixon, M.; Jortner, J. Electron Transfer—From Isolated Molecules to Biomolecules. *Adv. Chem. Phys.* **1999**, *106*, 35–202.
64. Marcus, R. A.; Sutin, N. Electron Transfer in Chemistry and Biology. *Biochim. Biophys. Acta* **1985**, *811*, 265–322.
65. Berlin, Y. A.; Hutchison, G. R.; Rempala, P.; Ratner, M. A.; Michl, J. Charge Hopping in Molecular Wires as a Sequence of Electron-Transfer Reactions. *J. Phys. Chem. A* **2003**, *107*, 3970–3980.
66. Voityuk, A. A., Computational Modeling of Charge Transfer in DNA. In *Computational Studies of RNA and DNA*; Šponer, J., Lankas, F., Eds.; Springer: Dordrecht, The Netherlands, 2006; pp 485−512.
67. Siriwong, K.; Voityuk, A. A.; Newton, M. D.; Rösch, N. Estimate of the Reorganization Energy for Charge Transfer in DNA. *J. Phys. Chem. B* **2003**, *107*, 2595–2601.
68. Ridley, J. E.; Zerner, M. C. An Intermediate Neglect of Differential Overlap Technique for Spectroscopy: Pyrrole and the Azines. *Theoret. Chim. Acta (Berlin)* **1973**, *32*, 111–134.
69. Kaufman, L.; Rousseeuw, P. J. *Finding Groups in Data: An Introduction to Cluster Analysis*; Wiley: New York, 1990.
70. Theodoridis, S.; Koutroumbas, K. *Pattern Recognition*, 3rd ed.; Academic Press, Inc.: Orlando, FL, USA, 2006.
71. Voityuk, A. A. Conformations of Poly(G)−Poly(C) π Stacks with High Hole Mobility. *J. Chem. Phys.* **2008**, *128*, 045104.
72. Troisi, A.; Nitzan, A.; Ratner, M. A. A Rate Constant Expression for Charge Transfer through Fluctuating Bridges. *J. Chem. Phys.* **2003**, *119*, 5782–5788.
73. Berlin, Y. A.; Grozema, F. C.; Siebbeles, L. D. A.; Ratner, M. A. Charge Transfer in Donor-Bridge-Acceptor Systems: Static Disorder, Dynamic Fluctuations, and Complex Kinetics. *J. Phys. Chem. C* **2008**, *112*, 10988–11000.
74. Rakotomalala, R. *TANAGRA Data Mining: A free software for research and academic purposes*, version 1.4.43; Lyon, France, 2012.
75. Lu, X. J.; Babcock, M. S.; Olson, W. K. Overview of Nucleic Acid Analysis Programs. *J. Biomol. Struct. Dyn.* **1999**, *16*, 833–843.
76. Olson, W. K.; Bansal, M.; Burley, S. K.; Dickerson, R. E.; Gerstein, M.; Harvey, S. C.; Heinemann, U.; Lu, X.-J.; Neidle, S.; Shakked, Z.; *et al*. A Standard Reference Frame for the Description of Nucleic Acid Base-Pair Geometry. *J. Mol. Biol.* **2001**, *313*, 229–237.
77. Venkatramani, R.; Keinan, S.; Balaeff, A.; Beratan, D. N. Nucleic Acid Charge Transfer: Black, White, and Gray. *Coord. Chem. Rev.* **2011**, *255*, 635–648.
78. He, W.; Hatcher, E.; Balaeff, A.; Beratan, D. N.; Gil, R. R.; Madrid, M.; Achim, C. Solution Structure of a Peptide Nucleic Acid Duplex from NMR Data: Features and Limitations. *J. Am. Chem. Soc.* **2008**, *130*, 13264–13273.
79. Voityuk, A. A. Electronic Coupling and on-Site Energies for Hole Transfer in DNA: Systematic Quantum Mechanical/Molecular Dynamic Study. *J. Chem. Phys.* **2008**, *128*, 115101.
80. Beveridge, D. L.; Barreiro, G.; Byun, K. S.; Case, D. A.; Cheatham, T. E.; Dixit, S. B.; Giudice, E.; Lankas, F.; Lavery, R.; Maddocks, J. H.; *et al*. Molecular Dynamics Simulations of the 136 Unique Tetranucleotide Sequences of DNA Oligonucleotides. I. Research Design and Results on D(C(P)G) Steps. *Biophys. J.* **2004**, *87*, 3799–3813.
81. Voityuk, A. A. Can Charge Transfer in DNA Significantly Be Modulated by Varying the π-Stack Conformation? *J. Phys. Chem. B* **2009**, *113*, 14365–14368.
82. Wang, J. M.; Cieplak, P.; Kollman, P. A. How Well Does a Restrained Electrostatic Potential (RESP) Model Perform in Calculating Conformational Energies of Organic and Biological Molecules? *J. Comput. Chem.* **2000**, *21*, 1049–1074.
83. Hobza, P.; Sponer, J. Structure, Energetics, and Dynamics of the Nucleic Acid Base Pairs: Nonempirical *Ab Initio* Calculations. *Chem. Rev.* **1999**, *99*, 3247–3276.
84. Lu, X.-J.; Olson, W. K. 3DNA: A Software Package for the Analysis, Rebuilding and Visualization of Three-Dimensional Nucleic Acid Structures. *Nucleic Acids Res.* **2003**, *31*, 5108–5121.
85. Peterson, B.; Nielsen, B. B.; Rasmussen, H.; Larsen, I. K.; Gajhede, M.; Nielsen, P. E.; Kastrup, J. S. Crystal Structure of a Partly Self-Complementary Peptide Nucleic Acid (PNA) Oligomere Showing a Duplex−Triplex Network. *J. Am. Chem. Soc.* **2005**, *127*, 1424–1430.
86. Rasmussen, H.; J., K. S.; Nielsen, J. N.; Nielsen, J. M.; Nielsen, P. E. Crystal Structure of a Peptide Nucleic Acid (PNA) Duplex at 1.7 a Resolution. *Nat. Struct. Biol.* **1997**, *4*, 98–101.
87. Eichert, A.; Behling, K.; Betzel, C.; Erdmann, V. A.; Fürste, J. P.; Förster, C. The Crystal Structure of an "All Locked" Nucleic Acid Duplex. *Nucleic Acids Res.* **2010**, *38*, 6729–6736.
88. Ivanova, A.; Rösch, N. The Structure of LNA:DNA Hybrids from Molecular Dynamics Simulations: The Effect of Locked Nucleotides. *J. Phys. Chem. A* **2007**, *111*, 9307–9319.
89. Vargason, J. M.; Henderson, K.; Ho, P. S. A Crystallographic Map of the Transition from B-DNA to A-DNA. *Proc. Natl. Acad. Sci. U.S.A.* **2001**, *98*, 7265–7270.
90. Guéron, M.; Demaret, J.-P.; Filoche, M. A Unified Theory of the B-Z Transition of DNA in High and Low Concentrations of Multivalent Ions. *Biophys. J.* **2000**, *78*, 1070–1083.
91. Moulaei, T.; Maehigashi, T.; Lountos, G. T.; Komeda, S.; Watkins, D.; Stone, M. P.; Marky, L. A.; Li, J.; Gold, B.; Williams, L. D. Structure of B-DNA with Cations Tethered in the Major Groove. *Biochemistry* **2005**, *44*, 7458–7468.
92. Řeha, D.; Voityuk, A. A.; Harris, S. A. An *in Silico* Design for a DNA Nanomechanical Switch. *ACS Nano* **2010**, *4*, 5737–5742.
93. Balaeff, A.; Craig, S. L.; Beratan, D. N. B-DNA to Zip-DNA: Simulating a DNA Transition to a Novel Structure with Enchanced Charge-Transport Characteristics. *J. Phys. Chem. A* **2011**, *115*, 9377–9391.
94. Kashimura, Y.; Nakashima, H.; Furukawa, K.; Torimitsu, K. Fabrication of Nano-Gap Electrodes Using Electroplating Technique. *Thin Solid Films* **2003**, *438 - 439*, 317–321.
95. Priyadarshy, S.; Risser, S. M.; Beratan, D. N. DNA Is Not a Molecular Wire: Protein-like Electron-Transfer Predicted for an Extended π-Electron System. *J. Phys. Chem.* **1996**, *100*, 17678–17682.
96. Fukui, K.; Tanaka, K. Distance Dependence of Photoinduced Electron Transfer in DNA. *Angew. Chem., Int. Ed.* **1998**, *37*, 158–161.
97. Kelley, S. O.; Barton, J. K. DNA-Mediated Electron Transfer from a Modified Base to Ethidium: π-Stacking as a Modulator of Reactivity. *Chem. Biol.* **1998**, *5*, 413–425.
98. Voityuk, A. A.; Rösch, N. Fragment Charge Difference Method for Estimating Donor−Acceptor Electronic Coupling: Application to DNA π-Stacks. *J. Chem. Phys.* **2002**, *117*, 5607–5616.
99. Voityuk, A. A. Assessment of Semiempirical Methods for the Computation of Charge Transfer in DNA π-Stacks. *Chem. Phys. Lett.* **2006**, *427*, 177–180.